

Photochemical & Photobiological Sciences

Accepted Manuscript



This is an *Accepted Manuscript*, which has been through the Royal Society of Chemistry peer review process and has been accepted for publication.

Accepted Manuscripts are published online shortly after acceptance, before technical editing, formatting and proof reading. Using this free service, authors can make their results available to the community, in citable form, before we publish the edited article. We will replace this *Accepted Manuscript* with the edited and formatted *Advance Article* as soon as it is available.

You can find more information about *Accepted Manuscripts* in the [Information for Authors](#).

Please note that technical editing may introduce minor changes to the text and/or graphics, which may alter content. The journal's standard [Terms & Conditions](#) and the [Ethical guidelines](#) still apply. In no event shall the Royal Society of Chemistry be held responsible for any errors or omissions in this *Accepted Manuscript* or any consequences arising from the use of any information it contains.

ARTICLE

Evidence of additional excitation energy transfer pathways in the phycobiliprotein antenna system of *Acaryochloris marina*

Cite this: DOI: 10.1039/x0xx00000x

Received 00th January 2012,
Accepted 00th January 2012

DOI: 10.1039/x0xx00000x

www.rsc.org/A.C. Nganou,^{a,b} L. David,^c N. Adir,^c D. Pouhe,^d M.J. Deen,^e and M. Mkandawire^a

To improve energy conversion efficiency of solar organic cell, the clue may lie in development of devices inspired by efficient light harvesting mechanism of some aquatic photosynthetic microorganisms adapted to low light intensity. Consequently, we investigated the pathways of excitation energy transfer (EET) from successive light harvesting pigments to the low energy level inside the phycobiliprotein antenna system of *Acaryochloris marina*, a cyanobacterium, using a time resolved absorption difference spectroscopy with a resolution time of 200 fs. The objective was to understand the actual biochemical process and pathways that determine the EET mechanism. Anisotropy of the EET pathway was calculated from the absorption change trace in order to determine the contribution of excitonic coupling. The results reveal a new electron energy relaxation pathway of 14 ps inside the phycocyanin component, which runs from phycocyanin to the terminal emitter. The bleaching of the 660 nm band suggests a broader absorption of the terminal emitter between 660 nm and 675 nm. Further, there are trimer depolarization kinetics of 450 fs and 500 fs in high and low ionic strength, respectively, which arise from the relaxation of the β_{84} and α_{84} in adjacent monomers of phycocyanin. Under conditions of low ionic strength buffer solution, the evolution of the kinetic amplitude during the depolarization of the trimer is suggestive of trimer conservation within the phycocyanin hexamer. The anisotropy values were 0.38 and 0.40 in high and in low ionic strength, respectively, indicating that there is no excitonic delocalization in high energy level of phycocyanin hexamers.

Introduction

Current trends of rising global energy demands compounded with diminishing fossil fuel resources and increasing environmental consciousness, have fuelled an on-going quest for alternative or renewable energy sources. One attractive solution is the conversion of sunlight into electric energy using low cost, easy-to-manufacture organic solar cells. Although these organic solar cells are becoming increasingly popular, their efficiency in converting solar into electricity remains very low, lying at 13.8%¹. One potential way to improve the organic solar cell's efficiency is to mimic the efficient light harvesting mechanism used in aquatic photosynthetic microorganisms that have adapted to environments with low sunlight conditions. One such organism is the cyanobacterium, *Acaryochloris marina*.

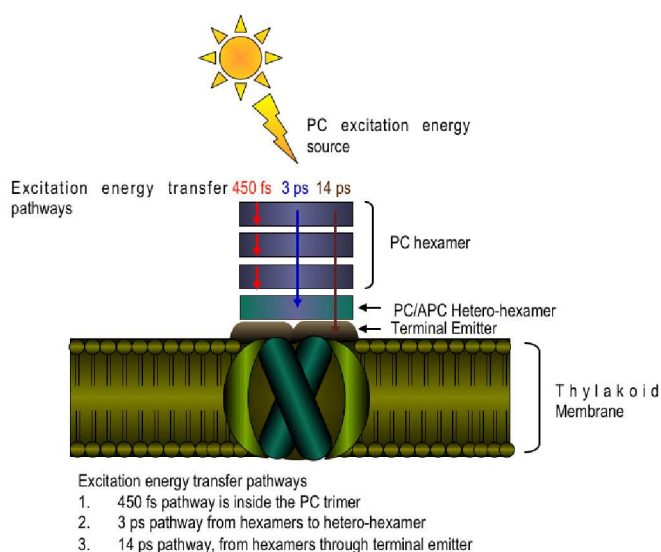
Unlike most cyanobacteria, which have chlorophyll *a* (*Chl a*) as the dominant light harvesting pigment, *A. marina* has

chlorophyll *d* (*Chl d*) as the dominant pigment for harvesting sunlight^{2,3}. In whole cells of *A. marina*, *Chl d* is observed at around 714-718 nm^{2,4}. Based on this finding, it has been always assumed that *Chl d*, by enabling utilization of the red light above 700 nm (not absorbed by organisms with *Chl a* as the main pigment), is responsible for the ability of *A. marina* to adapt to far-red light enriched environments where visible light intensity is low, but where far-red light is not decreased. Also, *A. marina* can contain small amounts of *Chl a* depending on its growth conditions⁵. Furthermore, *Chl d* has a lower redox potential than *Chl a*. Therefore, the ability of *A. marina* to adapt easily in environments with low light intensity cannot be attributed solely to its pigment organization. It is likely that other factors, such as the mechanism that governs excitation energy transfer (EET) in the organism, play an important role in *A. marina*'s light harvesting abilities.

To harvest light in the spectral gap where absorption via chlorophyll is low, *A. marina* uses phycobiliprotein (PBP) as an

outer antenna system^{6,7}. Located on the thylakoid membrane, PBP is a rod-like structure suggested to be composed of four stacked hexameric discs⁸. Three of the hexamers contain only phycocyanin (PC), while the fourth is a hetero-hexamer containing PC and allophycocyanin (APC), which have absorption bands at 618 and 640 nm, respectively⁸. The hexamer and heterohexamer are structurally organized by a connection of two trimers through C₃ symmetry⁹ (also see scheme 1). The EET in *A. marina* has been suggested to start after excitonic relaxation between α_{84} and β_{84} in approximate ~400 fs, which is followed by overall equilibration of PC dynamic in 3 ps. From that equilibration of the PC, the excitation energy was suggested to be transferred to APC in 3 ps, which is followed by a 14 ps EET from APC to the terminal pigment at 675 nm. The EET is further suggested to be funnelled to the photosystem (PSII) in 100 ps¹⁰.

kinetic of 10 ps component was in contradiction with the 3 ps of PC equilibration suggested by previous works¹⁰. From this observation, the only possibility of EET is a direct pathway from PC to the terminal emitter pigment. In absence of decay associate spectra from the ground state bleaching along all the energy level of the *A. marina* PBS, we were not able to support the idea that there is an effective additional channel of EET. In this work, we investigated the antenna system of *A. marina* PBS in high and low phosphate buffer at high energy level (i.e. PC), intermediate (i.e. APC) and low energy level (i.e. terminal emitter pigment). Using decay associate spectra of the ground state bleaching, we followed the energy pathway from PC to the terminal emitter pigment to verify whether or not the 14 ps is a viable EET that has its origin in PC before being transferred to the terminal emitter pigment. The change in phosphate concentration was used to gain insight the route of the slow kinetic (14 ps).



Scheme 1. Graphic abstract of the study showing the now known excitation energy transfer pathways in *A. marina*

Recently, it has been established that the excitation light harvesting by the phycobilisomes (PBS) in cyanobacteria is transferred to both reaction system (photosystem I (PS I) and II (PS II))¹¹. This is suggested to occur through two channels of EET, namely: One from the PBS to the PSII and the other from PBS to PSI. Suggesting that having an assembly sub-components distributed from the high energy level to low energy level, with an intermediate energy level between the high energy level and the low energy level does not guarantee that the excitation energy transfer will flow from high energy level throughout the intermediate level before reaching the low energy level. Further review on reaction centre mechanism can be found in reference therein.⁷

In view of this argument, we investigated whether or not the excitation energy transfer in the PBS of *A. marina* may flow from the PC to the terminal pigment at 665 nm with the same kinetic component. This hypothesis was inspired by the recent insight we gained in PC of *A. marina*, where the existence of a slow kinetic of 10 ps component was observed¹². This slow

Results and discussion

Comparison between absorption bands of PBP and PBS antenna systems

Previous studies of energy transfer kinetics in a phycobilisome (PBS) of *A. Marina* have shown absorption maximum at 618 nm, which is a known maximum absorption of the PC, while the sub-compound APC exhibits its absorption at 640 nm^{10,12}. However the kinetics in the phycobiliprotein (PBP) antenna complex of *A. marina* remains unstudied. Consequently, we investigated the PBP of *A. marina* and compared it to the PBS of *T. elongatus* to show that the differences between their PBS is attributed to the more red-shifted absorption of APC. We studied the absorbance of the PBP of *A. marina* across a range of wavelengths in both low and high ionic strength solutions; we also measured absorption in the PBS of *T. elongatus* (Figure 1). Figure 1a reveals that the spectra for both show PBP of *A. marina* and PBS of *T. elongatus* are very similar, which is obvious, except for the spectra shoulder at around 650 nm. The shoulder demonstrates the active absorption band of APC in the PBS of *T. elongatus*, while there appears no APC active absorption band of PBS in *A. marina*. Furthermore at blue-shifted wavelength, which is below 600 nm, the PBS of *A. marina* in low ionic strength displayed a slightly broader spectrum than in high ionic strength.

To investigate the details of the absorbance spectrums in these three biological systems, we computed the second derivative of absorbance vs. wavelength of the spectrum, allowing us to see fine details of their absorbance spectrum features (indicated by arrows in Figure 2b). Consequently, spectral absorption gap of APC becomes apparent in the PBP of *A. marina* at 640 nm. Similar finding was previously reported^{6,10}. Further, The spectral gap absorption of APC was observed at 650 nm in the PBS antenna system of *T. elongatus* and 640 nm in the PBP antenna system of *A. marina*. Further, the second derivative of the absorbance spectra reveals a 10 nm red-shift of the APC

assembly in the PBS antenna system of *T. elongatus*, which is observed at 650 nm in high ionic strength (Figure 1(b)). This difference is likely induced by the presence of more APC at 650 nm in the PBS of *T. elongatus* than in the PBP antenna system of *A. marina* at 640 nm, as well as the L_{CM} in the PBP system. The difference between PBP and PBS systems is most apparent in the short wavelength spectral range, especially when the PBS is compared to the PBP antenna system at low ionic strength. In the short wavelength spectral range, PBP has a broader spectrum than PBS (Figure 1). The increased difference is related to the procedure used to isolate the antenna system from the cyanobacteria, when the isolation of the antenna system is done in the absence of phosphate in buffer. This could be also responsible for differences observed in the red-shifted spectral gap that relates to the presence of the L_{CM} in PBS of *T. elongatus*.

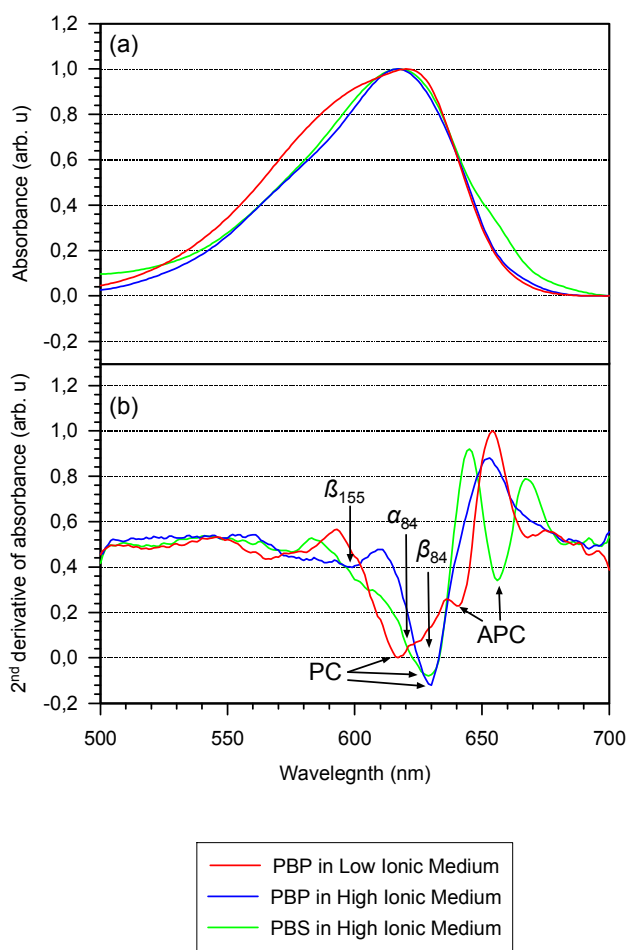


Fig 1. Absorption data for phycobilisome in the PBP antenna system of *A. marina* in high and in ionic mediums, and in the PBS antenna system of *T. elongatus*, shown as raw absorption spectra (a) and as the respective second derivative of absorbance, with particular proteins indicated (b). All spectra were obtained at RT

Further, the second derivative of the absorbance spectra reveals shouldered at 660 nm and 680 nm in the PBS antenna system *T. elongatus* (see Figure 2b), and the gap between these two

wavelengths is the band gap where the terminal emitter electronic state is expected to appear. The second derivative of the absorbance maximum of the rod PBP antenna shows that the PC and APC absorption maximum peaks are around 618 nm and 640 nm, respectively, which agrees with previous findings⁸. Both the PBS of *T. elongatus* and the PBP of *A. marina* have a shoulder at 570 nm, as revealed in the second derivative absorption spectrum. This may be due to a number of factors. One explanation is that this shoulder results from the differences in conformation among the cofactors, which affects the broadening of the absorption spectrum at low energy level. This effect is due to the cofactors' side chains of propanoic acid, which is very sensitive to changes in ionic strength of the solution. Therefore, the isolated PBS of *A. marina*, used in this work was consistent with previous results^{10 12}.

Excitation Energy Transfer from PC to terminal emitter pigment via APC

In order to show that the EET reaches the APC and the terminal pigment after excitation of the PC at 618 nm, we investigated their ground state bleaching of the APC and the terminal pigment at 640 nm and 665 nm. To accomplish this, samples of the isolated antenna systems of *A. marina* and *T. elongatus* were excited at 618 nm, and the decay kinetics were probed at different wavelengths from 625 to 665 nm. Here, we include the results for only four specific wavelengths that allowed comparison and contrast of the dynamics of the two model biological systems; the absorption characteristics of other wavelengths did not exhibit characteristics of interest and are therefore not included. The results for the selected wavelengths are shown in Figure 3. For all samples, the bleaching occurred immediately after excitation. This is because of the ground state depletion, which represents the dynamic relaxation from the excited to ground state. This is observed on the spectra at 625 nm and 650 nm for the PBS antenna system of *T. elongatus*, and at 625 nm and 640 nm for PBP antenna system of *A. marina*. The bleaching disappears at wavelengths above 655 nm, at which point an absorption rise appears (data not shown). The rise in the absorption trace is followed by a delayed bleaching (Figures 2). Thus, the replacement of the ground state depletion by the positive absorption suggests that the excited state population mainly originates from PC and not from APC. Furthermore, there are 660 nm trace decays within the 3 and 14 ps kinetic components. The presence of the 3 ps kinetic component indicates that the positive absorption trace is induced by the excited state absorption (ESA) of PC. The kinetic component of 14 ps, earlier found in APC, supports the previous suggestion that APC bleaches at a low energy level state^{12, 13}. Despite the different architectural design of the PBP and PBS antenna system, they both have the same ESA – although they occur at different absorption bands (660 nm and 665 nm, respectively). The delayed bleaching, which is below zero at 665 nm, marks the terminal emitter absorption in the PBS antenna system of *T. elongatus*. The L_{CM} linker protein has been proposed to be functional in the absorption gap where the terminal emitter is expected.¹⁴

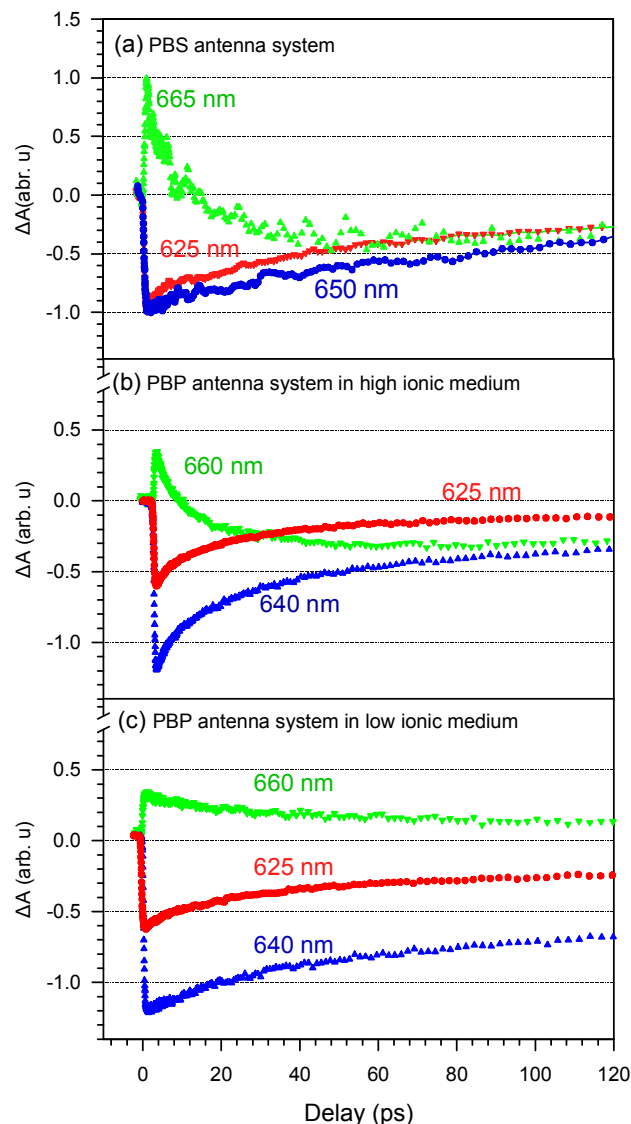


Fig 2. Trace of photo-induced absorption changes for three selected wavelengths each of the PBS antenna system of *T. elongatus* (625 nm, 650 nm and 665 nm represent the excited states of PC, APC and the linker core membrane, respectively) (a), the PBP antenna system of *A. marina* in high ionic strength (625 nm, 640 nm and 660 nm represent the excited states of PC, APC and the linker membrane pigment absorbing at 660 nm, respectively) (b), and the PBP antenna system of *A. marina* in low ionic strength (625 nm, 640 nm and 660 nm represent the excited states of PC, APC and the ESA of the PC, respectively) (c). Excitation was at 618 nm in all cases.

Depending on the ionic strength of the medium, the excited state dynamics of the component that absorbs at 660 nm will appear above or below the zero level (Figure 2b-c). At low ionic strength, it is more likely that the coupling between the APC energy level and the low energy level of the antenna system is disrupted, indicating that the energy is no longer being funnelled to the low electronic state of the rod PBP of *A. marina*. This happens despite the fact that there is no total decoupling of the high electronic energy state between PC and APC, suggesting that the energy is transferred through a

previously unknown kinetic component. This is apparent from the broad relaxation dynamics trace between PC and APC at low ionic strength compared to high ionic strength.

Excitation Energy Transfer Pathway

In order to follow the kinetic components inside the PBP antenna system of *A. marina* in high and low ionic strength mediums, the decay-associated spectra (DAS) were plotted for three lifetime components. For PC, APC and the terminal emitter pigment spectral components, the evolution of the amplitude lifetime component is shown as DAS for the rod PBP of *A. marina* at high and low ionic strength (Figure 3). The DAS consist of a global analysis of the available lifetime components found in the sample, enabling clear visualization of the spectral dynamics of the excited states of the system. When the wavelength-dependent form of the amplitude at each time constant rises from negative to positive, it can be interpreted as energy transfer, provided that the wavelength at which the amplitude crosses zero coincides with an absorbing electronic state. For each lifetime, we observe the evolution of the amplitude as a function of wavelength. The following results of global fit were acquired using a multi-exponential decay model:

$$A(\tau, \lambda) = \sum_{i=1}^n a_i(\lambda) e^{-\frac{\tau}{\tau_i}} \quad (1)$$

The kinetics at different wavelength intervals were fitted together with the common values of the lifetimes τ_i as a linked parameter; the wavelength dependent amplitude factor $a_i(\lambda)$ was set as a non-linked parameter. The best fit was obtained with three components – those with the lifetimes $\tau_1 = 3$ ps, $\tau_2 = 14$ ps and $\tau_3 > 200$ ps (up to the resolution time of 1 ns). The obtained spectra display the evolution of the EET transfer, suggesting the pathway of a possible model fitting the involved EET.^{10, 15}

Figure 3a shows the evolution of three lifetime components found inside a rod PBP of *A. marina* at high ionic strength. The 3 ps component exhibits a negative spectrum in the interval range of 605-643 nm and a positive spectrum in the range of 643-675 nm. The negative spectrum gap of the 3 ps component exhibits a minimum around 618 nm, which reflects the decay of the PC's excited state. The positive spectrum gap of the 3 ps component may have two different origins. It can be described as being primarily the result of decay of the ESA of PC, due to the decay of the ESA within 3 ps¹⁰ and the absence of absorption changes of APC above 655 nm. Alternatively, it has been suggested that, between 643 nm and 655 nm, the positive spectrum gap is due to an increasing relative ground state bleaching of APC¹⁰, which in turn results from the EET from PC to APC. It turns out that the evolution of the 3 ps component is the excitation energy equilibrated between a fraction of PC hexamers (which are not coupled to the terminal emitter) and the part of the APC that is inside the heterohexamer PC/APC. The 3 ps kinetic component is shorter than the EET from the PC-containing rods to the APC-core inside the PBP antenna system of other cyanobacteria species, which has been reported to occur within 17-18 ps^{10, 16, 17}. Contrary to the previously suggestion that 3 ps kinetic represent

the overall equilibration from PC to APC¹⁰, these current result, therefore, points to that the value of 3 ps component is the excitation energy from PC to APC.

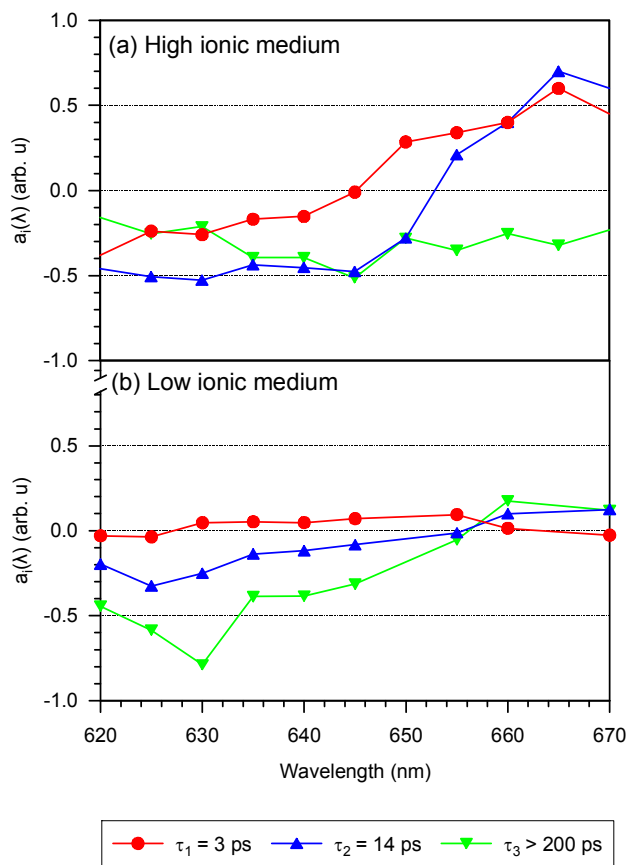


Fig. 3. Global analysis of the photo-induced absorption change traces of the PBP rod antenna system of *A. marina* in high ionic strength medium (a) and low ionic strength medium (b) after excitation at 618 nm. In each case, the kinetic amplitude course is shown within 3 ps, 14 ps and component more than 200 ps.

The 14 ps component (Figure 3a), like 3 ps, has a negative spectrum gap between 605–653 nm and a positive spectrum above 653 nm. It also exhibits a broad local minimum between 618–640 nm, where PC and APC have their maximum absorptions. The positive spectrum of 14 ps shows higher amplitude than that of the 3 ps component and exhibits a maximum at 670 nm. This increase in amplitude can, by analogy of the positive spectrum of 3 ps component between 643–655 nm, be attributed to increased ground state bleaching of the formation of the terminal emitter electronic state around 660–670 nm due to EET from PC/APC to the low electronic states of the rod PBP of *A. marina*. These differences likely reflect the red shift of the 14 ps decay component in comparison to the 3 ps component, indicating either an EET from the APC in PC/APC heterohexamer to the low electronic state of the rod PBP of *A. marina* around 660 - 675 nm or an EET from PC to that low electronic state. Due to the broad minimum of the spectrum for the 14 ps component, the possibility of an additional PC component contribution to this

kinetic cannot be excluded. By analogy to the terminal emitters in the PBS of other cyanobacteria^{18,19}, we suggest that the 660–675 nm electronic state in the rod PBP of *A. marina* could be similar to that of the linker core-membrane containing different pigments that connected the PBS of the cyanobacteria *T. elongatus* to the thylakoid membrane (figure 3a) and contributed to efficient energy transfer to Chl *d*²⁰. The same analogy extends to the 14 ps component identified inside APC with linker AP₆₆₅ in the PBS from *Mastigocladus laminosus*¹³, which raises the question of the particular structural assembly of the *A. marina* antenna system to photosystem II (PS II). Due to the isolated antenna system used here, the EET to the PS II is interrupted, leading to a long time constant of the excited state of the linker APC that is beyond the scale of our resolution. This lifetime exhibits a broad negative evolution in all spectral gaps, shown in Figure 3a as $\tau_3 > 200$ ps.

Figure 4b shows the evolution of three lifetime components found inside the rod PBP of *A. marina* in low ionic strength medium. As with high ionic strength medium, there are components with excitation kinetics of 3 ps, 14 ps and >200 ps. The 3 ps component exhibits an amplitude fluctuating close to zero such that it is likely to statistically average to zero. Therefore, the 3 ps component vanishes in low ionic strength because of its evolution close to the zero cross section of the DAS, meaning that the excited electronic states of PC and APC, via which the fast component of the energy is transferred, are decoupled at low ionic strength. Therefore, the equilibration reported previously¹⁰ is a fraction of the PC that is de-activated before its ground state relaxation. Consequently, it does not reflect the EET pathway from PC to the terminal emitter, but represents an intermediate equilibration state between PC and APC prior to the direct EET from PC to the terminal emitter.

The 14 ps component displays a negative spectrum from 620 nm to 653 nm and its spectrum is positive above 653 nm. It also exhibits a local minimum around 625 nm, which is near the absorption maximum of PC, and especially the PC chromophore α_{84} . The 14 ps component shows a reduction in amplitude that is most pronounced in the APC regime around 640 nm. The amplitude reduction in this range confirms the expectation that there is a fraction of an excited state lifetime originating from APC that is coupled to the terminal emitter (the low electronic state of the rod PBP). The remaining amplitude of the 14 ps component is suggested to be the fraction of excited state lifetime pigments originating from PC, which are directly coupled to the terminal emitter for EET. Thus, there is an excited electronic state fraction in rod PBP of *A. marina* which still couple to the low electronic state named terminal emitter of rod PBP of *A. marina* in low ionic strength solution. The above finding suggests that the 14 ps kinetic is also an intrinsic part of the PC electronic lifetime excited states. This reduction suggests that there is a fraction of PC populations that decay within the 14 ps component and transfer the energy with 14 ps time constant to the terminal emitter via APC electronic state. This PC population is hidden in high ionic strength because of the dominant population of the 3 ps component.

Finally, the evolution of the 14 ps kinetic component inside the rod PBP of *A. marina* in low ionic strength supports the conclusion that the excitation energy is equilibrated between a fraction of the PC hexamers and the low electronic state of the rod PBP via a fraction of the APC inside the heterohexamer PC/APC within 14 ps. This finding is in line with previous findings of lifetime components inside PC and APC that exhibited variations in the interval range of 10 – 18 ps^{16, 21}.

The τ_3 component (> 200 ps) exhibits a negative shape in the spectral gap between 620 and 653 nm. The slight positive amplitude above 653 nm might also be attributed to zero as a disruption of the 3 ps component. The minimum amplitude is located at 630 nm in the PC spectral range, which may be attributed to the phycocyanobilin chromophore β_{84} (Figure 3b). This may represent the excited state lifetime of PC, and has been found in other cyanobacteria to be in the ns range^{17, 22}. However, given the second minimum at 640 nm, it is likely that the APC state contributes to the long lifetime. This may represent the lifetime of the hetero-hexamer.

We can conclude from the results that the low ionic strength of the surrounding medium has strongly modified the electronic excited state of pigments in the whole antenna system. This modification enabled the visualisation of an excitation energy transfer from PC to the low electronic state of the rod PBP via APC in 14 ps.

The origin and existence of the 14 ps kinetic component in phycocyanin

For estimating the coupling between pigments with close spectral overlap, as well as energy transfer between these pigments, polarisation measurements were performed (Figure 4). The anisotropy decay that follows was measured and calculated from the direct trace of the absorption changes inside the intact and disrupted PBP rod of *A. marina*. Three components, with the depolarization time constants $\tau_1=280-500$ fs, $\tau_2=10-14$ ps and $\tau_3>200$ ps, were obtained (see Figure 4).

The results in this section reveal that the decay associated spectra and the sub-picosecond depolarisation decay observed inside the rod PBP antenna system of *A. marina* in high and low ionic strength media revealed new kinetics along the PC spectral gap. The anisotropy exhibits an initial value of 0.38 for the rod PBP of *A. marina* in high ionic strength and 0.4 for the rod PBP of *A. marina* in low ionic strength. The anisotropy decays with time constant components of 450 fs, 10 ps and > 200 ps for the rod PBP of *A. marina* in high ionic strength and with time constant components of 500 fs, 14 ps and > 200 ps in low ionic strength, which confirms the presence of the 14 ps component in PC.

Absorption changes and anisotropy in high and low ionic strength

Figure 4 shows the photo-induced absorption change traces inside the PBP rod of *A. marina* in high and low ionic strength after parallel and perpendicular excitation at 618 nm. As revealed by the parallel and perpendicular traces, the recovery

kinetics in low ionic strength in the rod PBP of *A. marina* are slower than those in high ionic strength. Each trace illustrates an initial rapid decay in transmission due to the saturation induced by the presence of the pump pulse. The amplitude of the absorption change trace is three times larger for the parallel trace than for the perpendicular trace. The trace of the rod PBP with different orientations (Figure 4a-b) yields a peak centred at 1.5 ps, at which point the saturation effect induced by the pump beam is terminated and relaxations of the dipole moment of pigments-pigments coupling take place. These couplings show a fast orientation relaxation of the dipole moment in high ionic strength medium (Figure 4a) compared to in low ionic strength medium. This observation appears with broader amplitude between the orientation relaxation of the dipole moment of the co-polarized parallel and perpendicular pump beams in low ionic strength (Figure 4b). These effects lead to the presence of a slow kinetic component.

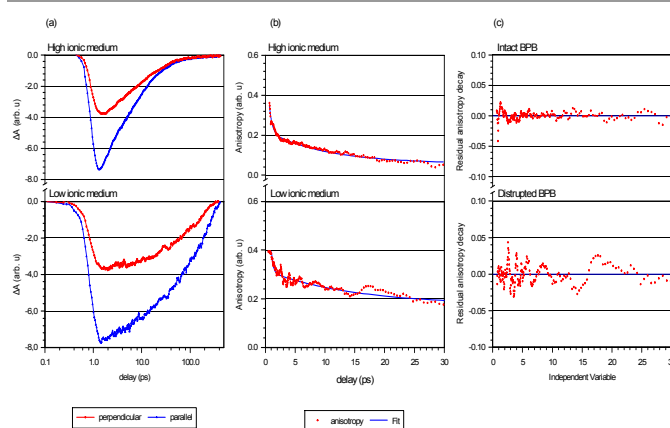


Fig. 4. (a) Comparison of parallel (||) and perpendicular (⊥) polarized absorption change of the rod PBP antenna system in high and low ionic medium after excitation and probe at 618 nm; (b) Anisotropy decay kinetics of the PBP antenna system in high and low ionic medium at room temperature; and (c) The residual of the anisotropy decay fit for intact and disrupted PBP antenna system.

This result fits with the earlier finding that the DAS component with kinetics of 14 ps originated from the PC. The fast recovery-delayed bleaching between excitations due to perpendicular and parallel pump beams in the absorption change is indicative of coupling induced by the high ionic strength medium (Figure 5a). This excited state population with a fast relaxation kinetic is absent in low ionic strength medium (Figure 5b), as with the disrupted 3 ps in the DAS (Figure 4b). Therefore, the EET occurs between parallel and perpendicular oriented electronic states (dipole moments) in the assembly of the PC hexamer in the rod PBP of *A. marina*. It appears that the change in ionic strength influenced the excited state of the dipole moment.

So far, we have analysed the influence of ionic strength of medium on pigment-pigment coupling, but have not estimated the time constant of these couplings. By subtracting the perpendicular trace data from the parallel trace data in equation 2, we remove the incoherent coupling present in the parallel trace, thus yielding the coherent coupling contribution between dipole moments in parallel polarisation. Dividing the latter

result by the total trace provides information on the anisotropy value; when this value is above or equal to 0.5 at room temperature, the exciton is thought to be delocalized among the pigments, as has been demonstrated by Edington et al.²³. The fit of the depolarisation trace with equation 3 yields the EET component of the coupling between dipole moment electronic states. This is shown in Figure 5b for the high ionic and low ionic mediums.

Figure 4b portrays the anisotropy decay with maximum values at 0.38 and 0.4 ($r(0)$). This measured anisotropy value which is close to the theoretical maximum of 0.4,²⁴ suggesting that no exciton is delocalized at the high energy level of the PC hexamer assembly in high and low ionic strength. Thus, there appears to be no excitonic delocalisation around all the excited pigments. In the case of an excitonic delocalisation, as previously described^{25, 26}, the anisotropy value would be located between 0.5 - 0.7; as a consequence, the exciton would be delocalised among the pigments that are far from the highest absorption state of PC assembly. Based on the anisotropy data presented here, that effect does not occur.

Three kinetic components of the excited state depolarization decay have been identified in high ionic strength medium: 450 fs, 10 ps and > 200 ps. The 450 fs kinetic might be induced by a fast excitonic relaxation of the dipole moment of the excitonically coupling chromophores α_{84} and β_{84} ²⁷ in the adjacent PC monomer. This 450 fs component fits within the existing proposed framework²⁸. Due to the 0.38 anisotropy value, we suggest that this value reflects EET between these chromophores to be trapped in the trimer.

EET within the single monomers occurs on a longer timescale as a result of the comparatively larger distance between adjacent chromophores. The kinetic is also close to that found by²⁹ in trimeric PC units. Thus, the higher amplitude of the 450 fs might be indicative of trimerization conservation, as well as excitonic coupling between adjacent chromophores α_{84} and β_{84} . The 10 ps component is in line with the 14 ps component found inside the assembly of the PC hexamer spectral range with the global analysis. This kinetic has been suggested to occur inside single hexamers²². According to the presence of homohexamer assembly units, and the maximum of the trimeric units in others species located around 617 nm²⁷, we suggest that the 618 nm component might be located around the maximum of the PC monomer in the trimer as well as the hexameric assembly units in the rod PBP of *A. marina*.

Thus, the excited state depolarisation decay in the trimer might occur within 10 ps. The non-negligible amplitude (13 %) of the kinetic of more than 200 ps indicates that a partial depolarization effect takes place between weakly coupled pigments. This residual anisotropy is an indication that the energy component around 10 ps is transferred out of the trimer, and consequently out of the hexamer prior to total depolarisation. This residual anisotropy, evident from the depolarisation trace (Figure 4c), can also be used as an indication of the symmetry order in the PC hexamer. This analysis confirms the expectation of a slow component kinetic in PC, which is transferred through the assembly of the

different hexamers to the linker membrane via APC in high ionic strength medium.

Figure 4 (d) shows the anisotropy decay with a maximum value of 0.4 in low ionic strength. The delay scale is cut off after 30 ps in order to get a better, less noisy view of the 14 ps component. This measured anisotropy value, which is equal to the theoretical maximum of 0.4, fits the same conclusion that was reached for high ionic strength: there is no delocalised exciton when the ionic strength is low. However, the decreased ionic strength did not affect the stability of the trimeric units, as evidenced by the high amount of 500 fs component. Comparing the 10 ps with 14 ps, we observed the decreased amplitude of the 14 ps component (Figure 5c-d), as resolved by the global analysis, suggesting that some of the excited state populations have disappeared. These excited-state populations are dominant in high ionic strength but vanish in low ionic strength, as the medium alters the coupling strength between different electronic states.

The high amplitude (40%) of the residual anisotropy leads to two conclusions. First, the 14 ps component propagation exits the trimeric units – and therefore the hexameric unit – before total depolarization of the trimer. Secondly, there is more asymmetry in the rod PBP antenna of *A. marina* at low ionic strength than there is at high ionic strength.

Furthermore, as previously described³⁰, the relaxation between two excitonic states that results from excitonic interaction between pigments in adjacent subunits of the PC trimer is best described by 450 fs in high ionic strength and by 500 fs in low ionic strength. However, those previous results were obtained using a laser system with time resolution of 1 ps. Additionally, that study found a 40 ps component, whereas we found two different time constant decays: 10 ps and 14 ps in high and low ionic strength, respectively. These two decays may originate from the pair of β chromophores in the adjacent monomer, rather than the pairs (β_1, α_3), (β_2, α_3) and (β_3, α_{3i}). The centre-to-centre distances of the pairs (β_1, α_3), (β_2, α_3), (β_3, α_{3i}) are greater than those of (β_1, β_2), (β_2, β_3), (β_3, β_1), which led to the longer time constants detected by Debreczeny and co-workers³⁰. In the absence of excitonic delocalisation, as indicated by the anisotropy values of 0.38 and 0.4 in high and low ionic strength, respectively, the 450 fs and 500 fs components are likely trapped in the hexamer, while the 10 and 14 ps components reflect transfer to the low electronic state in the rod PBP of *A. marina* via APC. Consequently, we suggest that this component is funnelled via β_{84} , which is located at the low energy level of the trimer. In conclusion, these finding gives full evidence of an additional pathway of EET as previously known, and suggest further that there may be more pathways of EET funneling.

Experimental

Sample Preparation

The *A. marina* strain MBIC11017 was grown in seawater K medium², while the cultures were grown at 26°C with filtered air bubbling and shaking. Continuous illumination was provided by a white fluorescence tube at light intensity of 20 μE ³¹. In order to carry out the femtosecond pump-probe experiment in mediums of varying ionic strength, the PBP antenna system was buffered with (high ionic strength) or without phosphate (low ionic strength). For femtosecond transient absorption changes, samples of the PBP antenna complex were put in a 2 mm optical path silica cuvette in which the concentration of the homogenized sample was measured on a conventional UV-Vis Spectrometer (Perkin-Elmer Lambda 19, Waltham Massachusetts, USA), such that an OD value of 1 at 618 nm could be maintained.

Femtosecond Pump – Probe Transient Absorption Spectroscopy

The femtosecond absorption measurements were performed using a commercial titanium sapphire system (Spectra – Physics Tsunami). A tuneable mode-locked titanium sapphire oscillator was used to generate pulses of 70 fs FWHM duration at 800 nm with a repetition rate of 82 MHz. The oscillator was pumped with a frequency-doubled continuous-wave Nd:YVO₄ laser (Millenia) running at power of 5W. The oscillator output was used to seed a regenerative Ti:sapphire amplifier (Spitfire), which was pumped by a power with pulse energy of 10 mJ and pulse duration of 200 ns. After recompression of the regenerative amplifier output, transformed and limited pulses of 1 mJ energy and 100 fs duration were obtained. The obtained output from Spitfire was used to pump a collinear optical parametric amplifier (OPA) to generate excitation pulses for any experiments in the visible and infrared spectral ranges. In this way, femtosecond pulses of 130 fs FWHM between 400 nm and 2.5 μm and energies of some ten micro Joules with a repetition rate of 1 kHz were achieved. For this experiment, the spectrum of the pump pulses was centred at 618 nm. The probe beam was obtained through generation of a white light by focusing a residual 800 nm from the OPA inside 1 cm optical path length flow cell containing D₂O. The white light is directed to a single grating pulse shaper³², where a 15 nm half bandwidth of a specific wavelength of the white light traps out in the focal plane of the pulse shaper with a time resolution of 200 fs and energy between 4 - 15 nJ/pulse³². In order to minimise annihilation, the experiment was performed at 4 nJ/pulse.

The probe and pump beam were superimposed in the sample at a cross section angle of 5°. To obtain decay associated spectra (DAS), the relative polarisation of the beams was set to an angle of 54.7° in order to avoid unwanted/misleading kinetics in the transient spectra caused by depolarization effects in the sample between the arrivals of the pump and the probe pulses. The transmitted probe beam and another 10% part of the probe beam trapped out in front of the sample and acting as a reference beam, were directed towards identical silicon photodiodes. Using a dual variable attenuator, the intensity of the two beams illuminating the photodiodes is set to identical values when the pump beam is blocked. Monitoring of the

transmitting probe beam through the sample was done by synchronously chopping the pump and probe beams at different frequencies with a mechanical chopper. The latter was phase-locked to the SR 510 Lock-In amplifier. The translation stage of 1 ns and the Lock-In amplifier were controlled by a computer, which was also used for data acquisition. The details and illustration of set-up has been outlined in Nganou et al.³³

Decay associated spectra of the ground state bleaching

The DAS consist of a global analysis of the available lifetime components found in the sample, enabling clear visualization of the spectral dynamics of the excited states of the system. When the wavelength-dependent form of the amplitude at each time constant rises from negative to positive, it can be interpreted as energy transfer, provided that the wavelength at which the amplitude crosses zero coincides with an absorbing electronic state. For each lifetime, we observe the evolution of the amplitude as a function of wavelength. The following results of global fit were acquired using a multi-exponential decay model:

$$A(\tau, \lambda) = \sum_{i=1}^n a_i(\lambda) e^{-\left(\frac{\tau}{\tau_i}\right)} + a_0 \quad (2)$$

The kinetics at different wavelength intervals were fitted together, with the common values of the lifetimes τ_i as a linked parameter; the wavelength dependent amplitude factor $a_i(\lambda)$ was set as a non-linked parameter.

Polarization Measurement

Absorption changes were monitored both with the polarization of the pump beam set parallel (ΔA_{\parallel}) to the polarised probe beam and with it set perpendicular (ΔA_{\perp}) to it. In all cases tested, the sum of ΔA_{\parallel} and $2\Delta A_{\perp}$ was indistinguishable from that obtained with isotropic monitoring with the pump beam polarization set at the optimum angle, 54.7°, with respect to probe beam (these measurements are not shown). A $\lambda/2$ -retarder of the pump laser's wavelength was employed to modulate the pump beam plane of polarization from parallel to perpendicular with respect to the parallel polarization of the probe beam. The anisotropy was calculated using the following function:

$$r(\tau) = \frac{\Delta A_{\parallel} - \Delta A_{\perp}}{\Delta A_{\parallel} + 2\Delta A_{\perp}} \quad (3)$$

The excited state lifetime decay of the depolarization pigments was fitted with a multi-exponential decay model:

$$A(\tau) = \sum_{i=1}^n a_i(\tau_i) e^{-\left(\frac{\tau}{\tau_i}\right)} + a_0 \quad (4)$$

The values of the depolarization time constant τ_i and the amplitude factor $a_i(\tau_i)$ were taken to be independent parameters.

Conclusions

The current results reveal the existence of previously unknown fast and slow kinetics in EET funnelling in PC of the rod PBP of *A. marina*. We have confirmed the details of this pathway using two different techniques. First, global analysis reveals the disappearance of the 3 ps component and the appearance of the 14 ps kinetic component of energy transfer between sub-

compounds. This finding was confirmed via the anisotropy, which shows the slow kinetics of the 10 ps and 14 ps components in PC at high and low ionic strength, respectively. It also revealed fast relaxation kinetics of 450 fs and 500 fs at high and low ionic strength, respectively, between α_{84} and β_{84} in adjacent the monomer of the trimer. The increased amplitude of this relaxation may be attributed to trimeric conservation. The residual anisotropy reveals the symmetry order inside the trimer by changing the amplitude of the 200 ps component. Furthermore, the anisotropy value close to 0.4 indicates that there is no excitonic delocalization in high energy level of PC among the three homo-hexamers of PC. The procedure of using both high and low ionic strength mediums is crucial to the identification of leading pathways, which may be dominant under some conditions but not others (e.g., the 14 ps component appears only at low ionic strength). When energy is efficiently transferred from a high energy level to the terminal emitter at low energy level, the excited state decay contribution of an intermediate sub-compound does not appear. This is evident from the EET between PC and the terminal emitter via APC in the 14 ps component of the rod PBP antenna system in low ionic strength. The 14 ps amplitude in the rod PBP antenna at low ionic strength than it is at high ionic strength, indicating that a fraction of the excited state decay is coupled to APC in the rod PBP antenna in high ionic strength. When the energy transfer is efficient, that fraction of the excited state is disrupted with the 3 ps, as observed in the rod PBP at low ionic strength.

Acknowledgements

Part of this work was done under DAAD research fellowship grants to Collins Nganou at TU Berlin. We thank Ms Sabine Kussin for cultivation of *A. marina*; and Ms Monica Wess for *A. marina* sample preparations. Finalisation of this work has been made possible with financial support from formally Enterprise Cape Breton Corporation (ECBC) to the Industrial Research Chair for Mine Water Management at Cape Breton University, and in kind support from Prof. David W. McCamant of Chemistry Department at University of Rochester.

Notes and references

^a Verschuren Centre for Sustainability in Energy and the Environment, Cape Breton University, P.O. Box 5300, 1250 Grand Lake Road, Sydney, Nova Scotia, Canada B1P 6L2.

^b Department of Chemistry, University of Rochester, RC Box 270216, Rochester, NY 14627-0216, USA.

^c Schulich Faculty of Chemistry, Technion- Israel Institute of Technology, Haifa, 32000 Israel.

^d Reutlingen University, Alteburgstraße 150, 72762 Reutlingen, Germany

^e Electrical and Computer Engineering, McMaster University, 1280 Main Street West Hamilton, Ontario, Canada L8S 4K1

1. J. Wallentin, N. Anttu, D. Asoli, M. Huffman, I. Åberg, M. H. Magnusson, G. Siefer, P. Fuss-Kailuweit, F. Dimroth, B. Witzigmann, H. Q. Xu, L. Samuelson, K. Deppert and M. T. Borgström, *Science*, 2013, 339, 1057-1060.
2. H. Miyashita, H. Ikemoto, N. Kurano, K. Adachi, M. Chihara and S. Miyachi, *Nature*, 1996, 383, 402-402.
3. C. Chen, W. Cai, M. Long, B. Zhou, Y. Wu, D. Wu and Y. Feng, *ACS Nano*, 2010, 4, 6425 - 6432.
4. A. W. D. Larkum and M. Kühl, *Trends in Plant Science*, 2005, 10, 355-357.
5. M. Akiyama, H. Miyashita, H. Kise, T. Watanabe, S. Miyachi and M. Kobayashi, *Analytical Sciences*, 2001, 17, 205-208.
6. Q. Hu, J. Marquardt, I. Iwasaki, H. Miyashita, N. Kurano, E. Morschel and S. Miyachi, *Biochimica Et Biophysica Acta-Bioenergetics*, 1999, 1412, 250-261.
7. E. Romero, R. Augulis, V. I. Novoderezhkin, M. Ferretti, J. Thieme, D. Zigmantas and R. van Grondelle, *Nat Phys*, 2014, 10, 676-682.
8. P. Apostoli, *Fresenius J Anal Chem*, 1999, 362, 499-504.
9. N. Adir, *Photosynthesis Research*, 2005, 85, 15-32.
10. C. Theiss, F.-J. Schmitt, J. Pieper, C. Nganou, M. Grehn, M. Vitali, R. Olliges, H. J. Eichler and H.-J. Eckert, *Journal of Plant Physiology*, 2011, 168, 1473-1487.
11. H. Liu, H. Zhang, D. M. Niedzwiedzki, M. Prado, G. He, M. L. Gross and R. E. Blankenship, *Science*, 2013, 342, 1104-1107.
12. C. Nganou, *The Journal of Chemical Physics*, 2013, 139, -.
13. A. R. Holzwarth, E. Bittersmann, W. Reuter and W. Wehrmeyer, *Biophysical journal*, 1990, 57, 133-145.
14. K.-H. Zhao, P. Su, S. Böhm, B. Song, M. Zhou, C. Bubenzer and H. Scheer, *Biochimica et Biophysica Acta (BBA) - Bioenergetics*, 2005, 1706, 81-87.
15. I. H. M. van Stokkum, D. S. Larsen and R. van Grondelle, *Biochimica et Biophysica Acta (BBA) - Bioenergetics*, 2004, 1657, 82-104.
16. J.-m. Zhang, J.-q. Zhao, L.-j. Jiang, X.-g. Zheng, F.-l. Zhao and H.-z. Wang, *Biochimica et Biophysica Acta (BBA) - Bioenergetics*, 1997, 1320, 285-296.
17. Å. Sandström, T. Gillbro, V. Sundström, R. Fischer and H. Scheer, *Biochimica et Biophysica Acta (BBA) - Bioenergetics*, 1988, 933, 42-53.
18. M. Mimuro, C. Lipschultz and E. Gantt, *Biochimica et Biophysica Acta (BBA) - Bioenergetics*, 1986, 852, 126-132.
19. D. J. Lundell and A. N. Glazer, *Journal of Biological Chemistry*, 1983, 258, 8708-8713.
20. Z. Petrasek, F.-J. Schmitt, C. Theiss, J. Huyer, M. Chen, A. Larkum, H. J. Eichler, K. Kemnitz and H.-J. Eckert, *Photochemical & Photobiological Sciences*, 2005, 4, 1016-1022.
21. T. Gillbro, Å. Sandström, V. Sundström, J. Wendler and A. R. Holzwarth, *Biochimica et Biophysica Acta (BBA) - Bioenergetics*, 1985, 808, 52-65.

22. A. R. Holzwarth, J. Wendler and G. W. Suter, *Biophysical journal*, 1987, 51, 1-12.
23. M. D. Edington, R. E. Riter and W. F. Beck, *The Journal of Physical Chemistry*, 1996, 100, 14206-14217.
24. J. R. Lakowicz, *Plasmonics*, 2006, 1, 5-33.
25. M. D. Edington, R. E. Riter and W. F. Beck, *J. Phys. Chem.*, 1995, 99, 5699-15704.
26. R. MacColl, *Biochimica et Biophysica Acta (BBA) - Bioenergetics*, 2004, 1657, 73-81.
27. M. P. Debreczeny, K. Sauer, J. Zhou and D. A. Bryant, *The Journal of Physical Chemistry*, 1993, 97, 9852-9862.
28. K. Sauer and H. Scheer, *Biochimica et Biophysica Acta (BBA) - Bioenergetics*, 1988, 157-170.
29. T. Gillbro, A. V. Sharkov, I. V. Kryukov, E. V. Khoroshilov, P. G. Kryukov, R. Fischer and H. Scheer, *Biochimica et Biophysica Acta (BBA) - Bioenergetics*, 1993, 1140, 321-326.
30. M. P. Debreczeny, K. Sauer, J. Zhou and D. A. Bryant, *The Journal of Physical Chemistry*, 1995, 99, 8420-8431.
31. M. Chen, M. Floetenmeyer and T. S. Bibby, *FEBS Letters*, 2009, 583, 2535-2539.
32. A. M. Weiner, *Review of Scientific Instruments*, 2000, 71, 1929-1960.
33. C. Nganou, L. David, R. Meinke, N. Adir, J. Maultzsch, M. Mkandawire, D. Pouhè and C. Thomsen, *The Journal of Chemical Physics*, 2014, 140, -.

